IEEE Access
Multidisciplinary ⋮ Rapid Review ⋮ Open Access Journal

Received September 4, 2018, accepted October 1, 2018, date of publication January 2, 2019, date of current version January 16, 2019.

Digital Object Identifier 10.1109/ACCESS.2018.2879972

Distributed Small-Signal Equivalent Circuit Model and Parameter Extraction for SiGe HBT

YABIN SUN[1], ZIYU LIU[2], XIAOJIN LI[1], AND YANLING SHI[1]
[1]Shanghai Key Laboratory of Multidimensional Information Processing, Department of Electrical Engineering, East China Normal University, Shanghai 200241, China
[2]State Key Laboratory of ASIC and System, School of Microelectronics, Fudan University, Shanghai 200433, China

Corresponding authors: Ziyu Liu (liuziyuyouxiang@sina.com) and Xiaojin Li (xjli@ee.ecnu.edu.cn)

This work was supported in part by the National Science and Technology Major Project under Grant 2016ZX02301003, in part by the National Natural Science Foundation of China under Grant 61574056 and Grant 61704056, in part by the Shanghai Sailing Program under Grant YF1404700, and in part by the Science and Technology Commission of Shanghai Municipality under Grant 14DZ2260800.

ABSTRACT In this paper, we present an improved high frequency small-signal distributed model for SiGe HBTs under forward-active mode based on the transmission line theory. The distributed nature of the transistor structure is taken into account in the proposed model. The single SiGe HBT is considered to be a cascade of many infinitesimal transistors, connected with the intrinsic base resistance. The closed-form solutions of admittance parameters for the distributed model are derived by solving the transmission line equation. With reasonable approximation and simplification, the model parameters are then directly extracted based on the nonlinear rational function fitting. The new improved distributed model and parameter extraction technique are validated with a $1 \times 1.2 \times 30\ \mu m^2$ SiGe HBT from 100 MHz to 20.89 GHz. The simulated S-parameters in the proposed transmission line model are in close agreement with the measured data, and the frequency characteristics of the transistors are well predicted.

INDEX TERMS Device modeling, small-signal model, parameter extraction, SiGe HBT, transmission line, rational function fitting

I. INTRODUCTION

Recently, SiGe HBTs have shown great potential in the future microwave or millimeter-wave applications [1], [2]. Accurate microwave model of SiGe HBTs is an important challenge in the reliable bipolar transistor circuit design. Small signal model is the footstone of the whole transistor microwave model, and therefore some commercial models, such as SGP, VBIC, HICUM and MEXTRAM, are developed for bipolar transistors [3], [4]. High frequency parasitic effect and non-quasi-static (NQS) effect are considered in these available compact models. As an optional part in HICUM or MEXTRAM, the distributed effect along the base region is one of the important high frequency effects at the microwave frequency range in bipolar transistors [5]–[7]. An effective base resistance described by a current source in series with an ideal base-emitter diode is used to model the distributed effect along the base region [8]. Depending on the different base structures, the effective base resistance is generally about 1/3 or 1/12 of the base finger resistance [9]. However, such a method lacks the flexibility to model the small signal characteristics at arbitrary high frequency. Similar to the case of MOSFET, the factor will deviate the ideal 1/3 or 1/12 as the operation frequency increases [10]. As for the parameter extraction method, most researches are primarily available for the lump compact models with numerical optimization or analytical calculation [11], [12], and fewer literatures are documented for the distributed network. Therefore, it is urgent to establish the accurate high frequency distributed model and parameter extraction technique for bipolar transistors.

Our previous research has discussed the distributed characteristics of SiGe HBTs under OFF-state and a simple lump voltage-controlled current source is used to mode the forward-active operation [13]. In this paper, the distributed concept is extended to the entire transistor network. To accurately describe the transient response, an improved high frequency distributed small-signal model is established for SiGe HBTs under forward-active operation. The transistor is divided into many infinitesimal elements, cascaded via the intrinsic base resistance. The admittance parameters are determined in a closed-form expression by solving transmission line equations. The small-signal model parameters under OFF-state and forward-active mode are then directly

2169-3536 © 2019 IEEE. Translations and content mining are permitted for academic research only.
Personal use is also permitted, but republication/redistribution requires IEEE permission.
See http://www.ieee.org/publications_standards/publications/rights/index.html for more information.

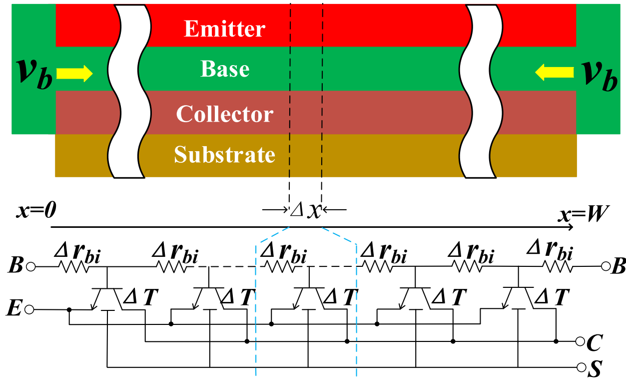

FIGURE 1. Demonstration of the distributed effect in a SiGe HBT transistor.

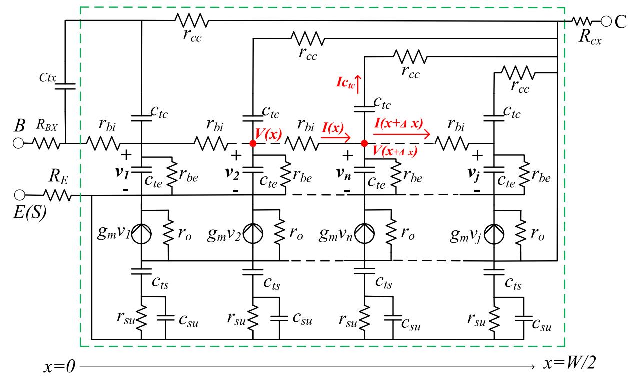

FIGURE 2. Small signal model of SiGe HBT, considering distributed effects.

extracted with the aid of nonlinear rational function fitting. The measured and simulated S-parameters are compared, and a good agreement is achieved under multi-bias points over the whole frequency range.

This paper is organized as follows. In Section II, a high frequency distributed small-signal model of SiGe HBT under forward-active mode is presented. The admittance parameters are then derived by solving the transmission line equations. In Section III, the model parameters in the proposed distributed model, including OFF-state and forward-active operation, are analytically extracted based on the non-linear rational function fitting. In Section IV, we apply the distributed model and extraction method to SiGe HBTs under different bias points, and the measured and simulated S-parameters are compared. Finally, the conclusions are drawn in Section V.

II. PROPOSED MODEL BASED ON DISTRIBUTED NETWORK

In first order approximation, the distributed effect along the base region is modeled with an effective intrinsic base resistance, denoted by R_{BI} and is calculated as [14]

$$R_{BI} = \frac{\rho_b W}{\eta L} \tag{1}$$

where ρ_b is the base sheet resistance, W and L are separately emitter width and length. η is a layout-dependent constant. For a rectangular emitter with only single base contact (layout of CBE), η equals 3, and η equals 12 when two base contacts on either side are adopted (layout of CBEBC). However, similar to the case of MOSFET, η also depends on the frequency, leading to a limitation and inaccuracy especially in microwave band [10]. Besides the distributed effect in intrinsic base region, the distributed effect also exists in collector and substrate. In this article, an improved high frequency distributed small-signal model based on the transmission line theory is proposed. The distributed network of SiGe HBTs with two base contacts is shown in Fig. 1. The whole transistor is considered to be a cascade of infinite number of infinitesimal elements, denoted by ΔT. Each element corresponds to the infinitesimal width of emitter, denoted by Δx. The internal base resistance connects each infinitesimal element.

The high frequency small signal model for above distributed network is shown in Fig. 2. Assuming that the electrical parameters are distributed uniformly along the base length direction, and the model parameters depicted in Fig. 2 are separately defined as

$$r_{bi} = \frac{R_{BI}\Delta x}{W} \tag{2}$$

$$c_{su} = \frac{C_{SU}}{W}\Delta x, \quad g_m = \frac{G_m}{W}\Delta x \tag{3}$$

$$c_{tj} = \frac{C_{Tj}}{W}\Delta x, \quad (j = c, e, s) \tag{4}$$

$$r_{cc} = \frac{R_{cc}W}{\Delta x}, \quad r_{su} = \frac{R_{su}W}{\Delta x}, \quad r_{be} = \frac{R_{be}W}{\Delta x}, \quad r_o = \frac{R_o W}{\Delta x} \tag{5}$$

where R_{BI}, C_{SU}, G_m, C_{Tc}, C_{Te}, C_{Ts}, R_{cc}, R_{su}, R_{be} and R_o are the total intrinsic base resistance, substrate bulk capacitance, transconductance, base-collector intrinsic capacitance, base-emitter intrinsic capacitance, substrate depletion capacitance, intrinsic collector resistance, substrate resistance, base-emitter diffusion resistance and output resistance, respectively.

To find the closed-form expression of the admittance parameters, the voltage $v(x)$ and current $i(x)$ at arbitrary position x should be first solved. For the sake of convenience, the emitter resistance R_E, extrinsic collector resistance R_{CX}, extrinsic base resistance R_{BX} and extrinsic base-collector capacitance C_{tx} are not included in the initial calculation. The distributed structure within the dashed box can be analyzed by the following transmission line equations:

$$\begin{cases} -\dfrac{di(x)}{dx} = v(x)y_{be} + (v(x) - V_C)y_{bc} \\ -\dfrac{dv(x)}{dx} = i(x)r_{bi} \end{cases} \tag{6}$$

where

$$y_{bc} = \frac{j\omega c_{tc}}{1 + j\omega c_{tc} r_{cc}} \tag{7}$$

$$y_{be} = j\omega c_{te} + \frac{1}{r_{be}} \tag{8}$$

The general solutions for $v(x)$ and $i(x)$ are expressed as

$$\begin{cases} v(x) = C_1 e^{\beta x} + C_2 e^{-\beta x} + \dfrac{y_{bc} V_C}{y_{bc} + y_{be}} \\ i(x) = -\dfrac{\beta}{r_{bi}}(C_1 e^{\beta x} - C_2 e^{-\beta x}) \end{cases} \tag{9}$$

where C_1, C_2 are the undetermined coefficients, and

$$\beta = \sqrt{(y_{bc} + y_{be}) r_{bi}} \tag{10}$$

The boundary conditions for SiGe HBs with the layout of CBEBC are given as

$$v(x)|_{x=0} = C_1 + C_2 + \frac{y_{bc} V_C}{y_{bc} + y_{be}} = V_B \tag{11}$$

$$v(x)|_{x=W} = C_1 e^{\beta W} + C_2 e^{-\beta W} + \frac{y_{bc} V_C}{y_{bc} + y_{be}} = V_B \tag{12}$$

Then we can reach

$$C_1 = (V_B - \frac{y_{bc} V_C}{y_{bc} + y_{be}}) \frac{1 - e^{-\beta W}}{e^{\beta W} - e^{-\beta W}} \tag{13}$$

$$C_2 = (V_B - \frac{y_{bc} V_C}{y_{bc} + y_{be}}) \frac{e^{\beta W} - 1}{e^{\beta W} - e^{-\beta W}} \tag{14}$$

Substituting (13) and (14) into (9), the following expressions for $v(x)$ and $i(x)$ are obtained

$$v(x) = (V_B - \frac{y_{bc} V_C}{y_{bc} + y_{be}})[\frac{sinh(\beta x) - sinh(\beta(x - W))}{sinh(\beta W)} + \frac{y_{bc} V_C}{y_{bc} + y_{be}}] \tag{15}$$

$$i(x) = -\frac{\beta}{r_{bi}}(V_B - \frac{y_{bc} V_C}{y_{bc} + y_{be}})[\frac{cosh(\beta x) - cosh(\beta(x - W))}{sinh(\beta W)}] \tag{16}$$

From (16), the terminal currents at base and collector contact are separately found as

$$i_B = 2i(0) = -\frac{2\beta}{r_{bi}}(V_B - \frac{y_{bc} V_C}{y_{bc} + y_{be}}) \frac{1 - \cosh(\beta W)}{\sinh(\beta W)} \tag{17}$$

$$i_C = (g_o + y_{cs} + y_{bc}) W V_C + (g_m - y_{bc}) \int_0^W v(x) dx \tag{18}$$

where

$$g_o = \frac{1}{r_o} \tag{19}$$

$$y_{cs} = \frac{j\omega c_{ts}(j\omega c_{su} + \frac{1}{r_{su}})}{j\omega c_{ts} + j\omega c_{su} + \frac{1}{r_{su}}} \tag{20}$$

The voltage integrating in (18) is calculated as

$$\int_0^W v(x) dx = \frac{y_{bc} W V_C}{y_{bc} + y_{be}} + \left(V_B - \frac{y_{bc} V_C}{y_{bc} + y_{be}}\right) \frac{2}{\beta} \frac{\cosh(\beta W) - 1}{\sinh(\beta W)} \tag{21}$$

Then the admittance parameters can be easily obtained and are separately given as

$$Y_{11} = \frac{2i(0)}{V_B}|_{V_C=0} = 2(y_{bc} + y_{be}) W \frac{\cosh(\beta W) - 1}{\beta W \sinh(\beta W)} \tag{22}$$

$$Y_{12} = \frac{2i(0)}{V_C}|_{V_B=0} = -2 y_{bc} W \frac{\cosh(\beta W) - 1}{\beta W \sinh(\beta W)} \tag{23}$$

$$Y_{21} = \frac{i_C}{V_B}|_{V_C=0} = 2(g_m - y_{bc}) W \frac{\cosh(\beta W) - 1}{\beta W \sinh(\beta W)} \tag{24}$$

$$Y_{22} = \frac{i_C}{V_C}|_{V_B=0} = (g_o + y_{cs} + y_{bc}) W + \frac{y_{bc}(g_m - y_{bc})}{y_{bc} + y_{be}} W \left[1 - 2\frac{\cosh(\beta W) - 1}{\beta W \sinh(\beta W)}\right] \tag{25}$$

The distributed effects in the actual transistor structure are reflected by the term of $\frac{\cosh(\beta W)-1}{\beta W \sinh(\beta W)}$. However, one should bear in mind that the extrinsic base-collector capacitance C_{tx} is not included in above calculation. When C_{tx} is considered, one can easily get the following admittance parameters

$$Y_{11} = 2(Y_{bc} + Y_{be}) \frac{\cosh(\beta W) - 1}{\beta W \sinh(\beta W)} + j\omega C_{tx} \tag{26}$$

$$Y_{12} = -2 Y_{bc} \frac{\cosh(\beta W) - 1}{\beta W \sinh(\beta W)} - j\omega C_{tx} \tag{27}$$

$$Y_{21} = 2(G_m - Y_{bc}) \frac{\cosh(\beta W) - 1}{\beta W \sinh(\beta W)} - j\omega C_{tx} \tag{28}$$

$$Y_{22} = \frac{Y_{bc}(G_m - Y_{bc})}{Y_{bc} + Y_{be}} \left[1 - 2\frac{\cosh(\beta W) - 1}{\beta W \sinh(\beta W)}\right] + j\omega C_{tx} + G_o + Y_{cs} + Y_{bc} \tag{29}$$

where

$$Y_{jk} = y_{jk} W \quad (jk = bc, be, cs) \tag{30}$$

$$G_m = g_m W \tag{31}$$

$$G_o = g_o W \tag{32}$$

In order to extract the model parameters in above admittance parameters, the hyperbolic function $\frac{\cosh(\beta W)-1}{\beta W \sinh(\beta W)}$ should be appropriately simplified. According to Taylor-series expansion, there exists

$$\frac{\cosh(x) - 1}{x \sinh(x)} \approx \frac{1}{2} - \frac{x^2}{24} + \frac{x^4}{240} - \frac{17x^6}{40320} + \frac{31x^8}{725760} + O[x]^8 \tag{33}$$

Here the first two terms in (33) are chosen, and the modified term $\frac{\cosh(\beta W)-1}{\beta W \sinh(\beta W)}$ can be simplified as

$$\frac{\cosh(\beta W) - 1}{\beta W \sinh(\beta W)} \approx \frac{1}{2} - \frac{(\beta W)^2}{24} = \frac{1}{2} - \frac{(Y_{bc} + Y_{be}) R_{bi}}{24} \tag{34}$$

Certainly, more adopted items in (33) will determine the more general equivalent circuit. However, the corresponding parameters extraction is more complicated and therefore we avoid doing this. Then the admittance parameters in (26)-(29) are separately reduced to

$$Y_{11} = (Y_{bc} + Y_{be})(1 - \frac{(Y_{bc} + Y_{be}) R_{bi}}{12}) + j\omega C_{tx} \tag{35}$$

$$Y_{12} = -Y_{bc}(1 - \frac{(Y_{bc} + Y_{be}) R_{bi}}{12}) - j\omega C_{tx} \tag{36}$$

$$Y_{21} = (G_m - Y_{bc})(1 - \frac{(Y_{bc} + Y_{be}) R_{bi}}{12}) - j\omega C_{tx} \tag{37}$$

$$Y_{22} = \frac{Y_{bc}(G_m - Y_{bc})R_{bi}}{12} + G_o + Y_{cs} + Y_{bc} + j\omega C_{tx} \quad (38)$$

Of course one can also calculate a higher order corrections in (33), and try to find a more general fitting to (26)-(29). But here we will not do so, since the obtained admittance parameters will be more complicated and it is difficult to extract the corresponding model parameters.

After converting the above obtained admittance matrix into impedance matrix, the two remained lumped parameter R_E and R_{CX} are easily added and then the final impedance matrix can be determined. The final detailed impedance matrix is not shown here, since R_E and R_{CX} can be easily extracted from forward Gummel method and Rcc_active method in advance [15], [16], respectively. They can be considered as constants and removed from the measured S-parameters, which would greatly simplify the parameter extraction procedure. In the following Section III, we will discuss the small-signal model parameter extraction.

III. SMALL-SIGNAL Model parameter extraction

A. CUT-OFF MODE (OFF-STATE)

The small-signal model parameters under cut-off mode are first extracted. Under this bias condition, G_m and G_o are approximately zero. From the forward-Gummel method and conventional Rcc_active method [15], [16], the extrinsic lump resistance R_E and R_{CX} can be extracted and removed from the measured S-parameters. Then the admittance parameters within the dashed box in Fig. 2 are reduced to

$$Y_{11} = (Y_{bc} + Y_{be})(1 - \frac{(Y_{bc} + Y_{be})R_{bi}}{12}) + j\omega C_{tx} \quad (39)$$

$$Y_{12} = Y_{21} = -Y_{bc}(1 - \frac{(Y_{bc} + Y_{be})R_{bi}}{12}) - j\omega C_{tx} \quad (40)$$

$$Y_{22} = -\frac{{Y_{bc}}^2 R_{bi}}{12} + Y_{cs} + Y_{bc} + j\omega C_{tx} \quad (41)$$

Combining (39)-(41), the real part and imaginary part of related admittance parameters can be derived as a rational function of angular frequency ω, and are separately given as

$$Im(Y_{11} + Y_{12}) = \frac{N_{10}\omega + N_{11}\omega^3}{1 + M_{11}\omega^2} \quad (42)$$

$$Re(Y_{11} + Y_{12}) = \frac{N_{20}\omega^2 + N_{21}\omega^4}{1 + M_{11}\omega^2} \quad (43)$$

$$Im(-Y_{12}) = \frac{N_{30}\omega + N_{31}\omega^3 + N_{32}\omega^5}{1 + M_{31}\omega^2 + M_{32}\omega^4} \quad (44)$$

$$Re(-Y_{12}) = \frac{N_{40}\omega^2 + N_{41}\omega^4}{1 + M_{31}\omega^2 + M_{32}\omega^4} \quad (45)$$

$$Im(Y_{12} + Y_{22}) = \frac{N_{50}\omega + N_{51}\omega^3 + N_{52}\omega^5}{1 + M_{31}\omega^2 + M_{32}\omega^4} \quad (46)$$

$$Re(Y_{12} + Y_{22}) = \frac{N_{60}\omega^2 + N_{61}\omega^4}{1 + M_{31}\omega^2 + M_{32}\omega^4} \quad (47)$$

where the lowest order terms' coefficients N_{i0} are written as

$$N_{10} = C_{te} \quad (48)$$

$$N_{20} = \frac{R_{bi}}{12} C_{te}(C_{tc} + C_{te}) \quad (49)$$

$$N_{30} = C_{tc} + C_{tx} \quad (50)$$

$$N_{40} = C_{tc}[(C_{te} + C_{tc})\frac{R_{bi}}{12} + R_{cc}C_{tc}] \quad (51)$$

$$N_{50} = C_{ts} \quad (52)$$

$$N_{60} = {C_{ts}}^2 R_{su} - \frac{R_{bi}}{12} C_{tc}C_{te} \quad (53)$$

Other coefficients are also a function of model parameters under cut-off mode and the detailed expressions are not shown here. By combining the respective real and imaginary parts of the above admittance parameters, some additional information could be transformed into new lowest order terms coefficients in the numerator and become available. Here, we define two variables

$$g_1 = N_{10}Re(Y_{11} + Y_{12}) - N_{20}\omega Im(Y_{11} + Y_{12}) \quad (54)$$

$$g_2 = N_{60}\omega Im(Y_{12} + Y_{22}) - N_{50}Re(Y_{12} + Y_{22}) \quad (55)$$

Then equations (54) and (55) can be rearranged as

$$g_1 = \frac{N_{70}\omega^4}{1 + M_{11}\omega^2} \quad (56)$$

$$g_2 = \frac{N_{80}\omega^4 + N_{81}\omega^6}{1 + M_{31}\omega^2 + M_{32}\omega^4} \quad (57)$$

where

$$N_{70} = \frac{R_{bi}}{12} {C_{tc}}^2 {C_{te}}^2 [\frac{R_{bi}}{12}(C_{te} + C_{tc}) - C_{tc}R_{cc}]R_{cc} \quad (58)$$

$$N_{80} = A_1 {C_{su}}^2 + B_1 C_{su} + C_1 \quad (59)$$

The coefficients A_1, B_1 and C_1 are given as

$$A_1 = {C_{ts}}^3 {R_{su}}^3$$

$$B_1 = (\frac{R_{bi}}{12} C_{tc}C_{te} + {C_{ts}}^2 R_{su}){C_{ts}}^2 {R_{su}}^2$$

$$C_1 = \frac{R_{bi}}{12} C_{tc}C_{te}[(C_{tc}R_{cc} + C_{ts}R_{su}){C_{ts}}^2 R_{su} - (\frac{R_{bi}C_{te}}{12} + C_{ts}R_{cc}){C_{tc}}^2 R_{cc}] \quad (60)$$

The coefficients N_{i0} (i $= 1 \sim 8$) can be separately determined from the nonlinear rational function fitting to (42)-(47) and (54)-(55). The typical fitting results for a $1 \times 1.2 \times 30\ \mu\text{m}^2$ SiGe HBT under $V_{BE} = -1$ V and $V_{CE} = 0$ V are shown in Fig. 3. An excellent agreement between the measured and fitted data over the whole frequency range is observed. The coefficients N_{i0} (i = 1-8) with narrow confidence interval are obtained accurately and shown in Table 1.

Compared to the conventional capacitance extraction from the linear fitting of cold Y-parameter (i.e., low frequency approximation) [17], the proposed method here can be viewed as a general broadband approach. For example, in the low frequency range (42), (44) and (46) can be reduced to

$$\frac{Im(Y_{11} + Y_{12})}{\omega}|_{at\ low\ frequency} \approx P_{10} = C_{te} \quad (61)$$

$$\frac{Im(-Y_{12})}{\omega}|_{at\ low\ frequency} \approx P_{30} = C_{tc} + C_{tx} \quad (62)$$

$$\frac{Im(Y_{12} + Y_{22})}{\omega}|_{at\ low\ frequency} \approx P_{50} = C_{ts} \quad (63)$$

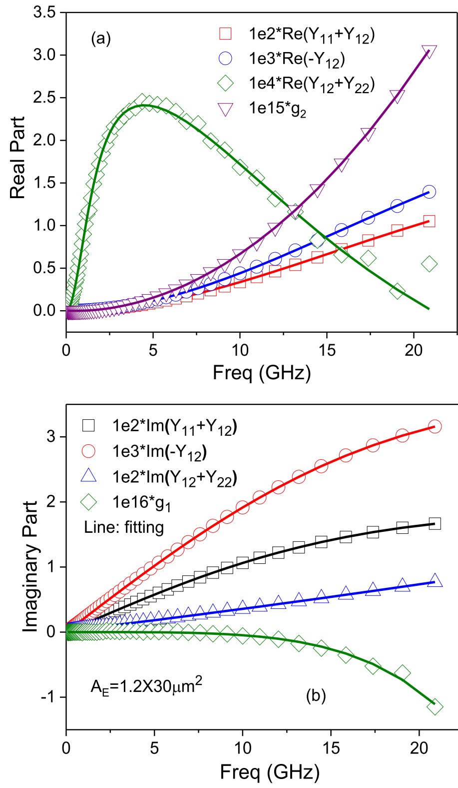

FIGURE 3. Measured (symbol) and fitted (line) data of (42)-(47) and (54)-(55) for a 1 × 1.2 × 30 μm^2 SiGe HBT under $V_{BE} = -1$ V and $V_{CE} = 0$ V.

TABLE 1. The fitted coefficients N_{i0} and confidence interval for 1 × 1.2 × 30 μm^2 SiGe HBT under $V_{BE} = -1$ V and $V_{CE} = 0$ V.

Vari.	Value	Confidence Intervals
N_{10} (1×10^{-13} F)	1.884	(1.883, 1.886)
N_{20} (1×10^{-24} Ω F^2)	0.95796	(0.9533, 0.9626)
N_{30} (1×10^{-13} F)	0.33165	(0.3312, 0.3321)
N_{40} (1×10^{-24} Ω F^2)	0.12492	(0.1236, 0.1263)
N_{50} (1×10^{-13} F)	0.85062	(0.8424, 0.8589)
N_{60} (1×10^{-24} Ω F^2)	3.0355	(2.918, 3.153)
N_{70} (1×10^{-61} Ω^3 F^5)	-2.9317	(-3.278, -2.586)
N_{80} (1×10^{-57} Ω^3 F^5)	1.8743	(1.758, 1.991)

which is the typical result in the low frequency approximation method. The comparison between the conventional and proposed method is presented in Fig. 4. As the measurement frequency increases, an obvious deviation appears in the low frequency approximation method.

By combining (48)-(53) and (58)-(59), the small-signal model parameters can be directly extracted as

$$R_{bi} = \frac{-B_2 + \sqrt{{B_2}^2 - 4A_2C_2}}{2A_2}$$

$$A_2 = {N_{10}}^4(2N_{20} + N_{40})(N_{20} + N_{40})$$

$$B_2 = -12{N_{10}}^2(4{N_{20}}^3 + 3{N_{20}}^2N_{40} + N_{10}N_{70})$$

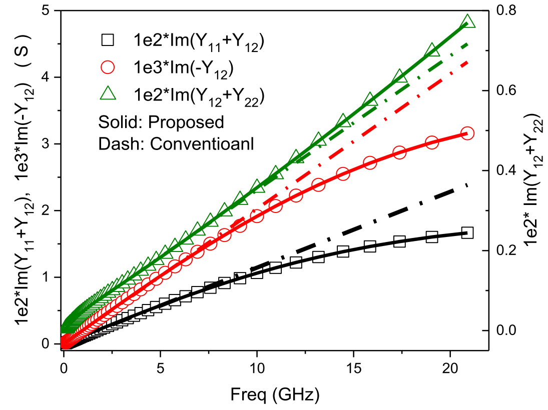

FIGURE 4. Comparison of conventional low frequency approximation and proposed non-linear rational function fitting method for a 1 × 1.2 × 30 μm^2 SiGe HBT under $V_{BE} = -1$ V and $V_{CE} = 0$ V.

$$C_2 = 144N_{20}(2{N_{20}}^3 + N_{10}N_{70}) \tag{64}$$

$$C_{te} = N_{10} \tag{65}$$

$$C_{tc} = \frac{12N_{20}}{N_{10}R_{bi}} - N_{10} \tag{66}$$

$$C_{tx} = N_{10} + N_{30} - \frac{12N_{20}}{N_{10}R_{bi}} \tag{67}$$

$$R_{cc} = \frac{R_{bi}[{N_{10}}^2R_{bi}(N_{40} + N_{20}) - 12{N_{20}}^2]}{(12N_{20} - {N_{10}}^2R_{bi})^2} \tag{68}$$

$$C_{ts} = N_{50} \tag{69}$$

$$R_{su} = \frac{12(N_{20} + N_{60}) - {N_{10}}^2R_{bi}}{12{N_{50}}^2} \tag{70}$$

$$C_{su} = \frac{-B_1 + \sqrt{{B_1}^2 - 4A_1(F_1 - N_{80})}}{2A_1} \tag{71}$$

Here the model parameters under cut-off mode have been directly determined by analytical expressions. After de-embedding the extracted extrinsic parameters, the intrinsic HBT network will be reached and the detailed extraction procedure will be discussion in the following section.

B. NORMAL-OPERATION (FORWARD-ACTIVE OPERATION)

The substrate-network and BC junction generally operates at reversed-biased in the normal-operated transistor. The bias dependence of substrate parameters (C_{ts}, C_{su} and R_{su}) and extrinsic C_{tx} can be easily obtained from above cut off operation, and then can be removed from the measured S-parameters. As a consequence, the admittance parameters for the remaining intrinsic HBT network can be separately re-arranged as

$$Im(Y_{11} + Y_{12}) = \frac{P_{10}\omega + P_{11}\omega^3}{1 + Q_{11}\omega^2} \tag{72}$$

$$Re(Y_{11} + Y_{12}) = \frac{P_{20} + P_{21}\omega^2 + P_{22}\omega^4}{1 + Q_{11}\omega^2} \tag{73}$$

$$Im(-Y_{12}) = \frac{P_{30}\omega + P_{31}\omega^3 + P_{32}\omega^5}{1 + Q_{31}\omega^2 + Q_{32}\omega^4} \tag{74}$$

TABLE 2. The fitted coefficients P_{i0} and confidence interval for $1 \times 1.2 \times 30\ \mu m^2$ SiGe HBT under $V_{BE} = 0.875$ V and $V_{CE} = 3$ V.

Vari.	Value	Confidence Intervals
P_{10} (1×10^{-13} F)	6.6814	(6.681, 6.682)
P_{20} (1×10^{-2} S)	0.12	(0.1159, 0.1236)
P_{30} (1×10^{-13} F)	0.26756	(0.2675, 0.2676)
P_{40} (1×10^{-25} Ω F^2)	1.0512	(1.05, 1.052)
P_{50} (1×10^{-12} F)	-2.4788	(-2.479, -2.478)
P_{60} (S)	0.1267	(1.263, 1.269)
P_{70} (1×10^{-13} F)	0.18945	(0.1891, 0.1899)
P_{80} (1×10^{-5} S)	9.2242	(9.224, 9.225)

$$Real(-Y_{12}) = \frac{P_{40}\omega^2 + P_{41}\omega^4}{1 + Q_{31}\omega^2 + Q_{32}\omega^4} \quad (75)$$

$$Im(Y_{21} - Y_{12}) = \frac{P_{50}\omega + P_{51}\omega^3 + P_{52}\omega^5}{1 + Q_{51}\omega^2} \quad (76)$$

$$Real(Y_{21} - Y_{12}) = \frac{P_{60} + P_{61}\omega^2 + P_{62}\omega^4}{1 + Q_{51}\omega^2} \quad (77)$$

$$Im(Y_{12} + Y_{22}) = \frac{P_{70}\omega + P_{71}\omega^3 + P_{72}\omega^5}{1 + Q_{71}\omega^2 + Q_{72}\omega^4} \quad (78)$$

$$Real(Y_{12} + Y_{22}) = \frac{P_{80} + P_{81}\omega^2 + P_{82}\omega^4 + P_{83}\omega^6}{1 + Q_{71}\omega^2 + Q_{72}\omega^4} \quad (79)$$

where the lowest order terms' coefficients P_{i0} are given as

$$P_{10} = C_{te} - \frac{R_{bi}(2C_{te} + C_{tc})}{12R_{be}} \quad (80)$$

$$P_{20} = \frac{1}{R_{be}}(1 - \frac{R_{bi}}{12R_{be}}) \quad (81)$$

$$P_{30} = C_{tx} + C_{tc}(1 - \frac{R_{bi}}{12R_{be}}) \quad (82)$$

$$P_{40} = C_{tc}[C_{te}\frac{R_{bi}}{12} + C_{tc}\left(\frac{R_{bi}}{12} + R_{cc}(1 - \frac{R_{bi}}{12R_{be}})\right)] \quad (83)$$

$$P_{50} = -G_{mo}[(C_{tc} + C_{te})\frac{R_{bi}}{12} + (1 - \frac{R_{bi}}{12R_{be}})\tau] \quad (84)$$

$$P_{60} = G_{mo}(1 - \frac{R_{bi}}{12R_{be}}) \quad (85)$$

$$P_{70} = C_{tc}(\frac{1}{R_{be}} + G_{m0})\frac{R_{bi}}{12} \quad (86)$$

$$P_{80} = G_o \quad (87)$$

Similar to the case under cutoff state, P_{i0} (i = 1-8) can be also accurately determined from the nonlinear rational function fitting of (72)-(79) verse ω. The typical fitting results for a $1 \times 1.2 \times 30\ \mu m^2$ SiGe HBT biased at $V_{BE} = 0.875$ V and $V_{CE} = 3$ V are shown in Fig. 5, from which an excellent agreement is found over the whole frequency range. The fitted coefficients P_{i0} (i = 1-8) with narrow confidence interval are simultaneously obtained, as depicted in Table 2.

When the constants P_{i0} (i-8) are determined, by combining (80)-(87), all the circuit elements in the normal-operated transistor can be extracted according to the following formulas

$$G_o = P_{80} \quad (88)$$

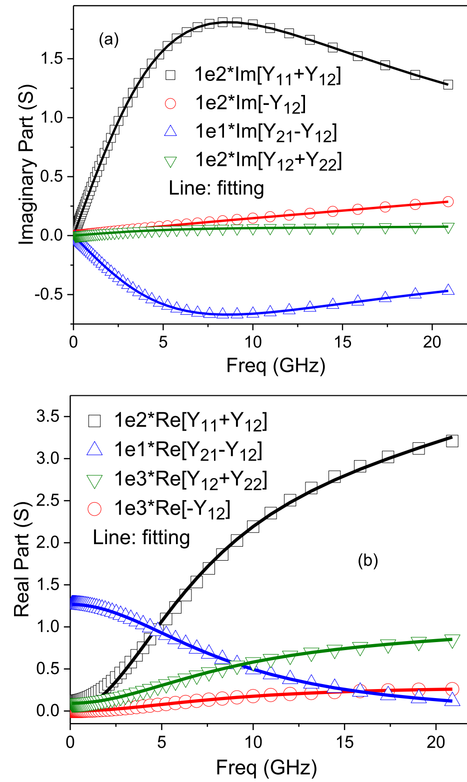

FIGURE 5. Measured (symbol) and fitted (line) data of (72)-(79) for a $1 \times 1.2 \times 30\ \mu m^2$ SiGe HBT biased at $V_{BE} = 0.875$ V and $V_{CE} = 3$ V.

$$G_{m0} = \frac{P_{60}P_{70}}{(P_{30} - C_{tx})(1 + \frac{P_{60}}{P_{20}})} + P_{60} \quad (89)$$

$$R_{be} = \frac{P_{60}}{G_{m0}P_{20}} \quad (90)$$

$$R_{bi} = \frac{12(G_{m0} - P_{60})P_{60}}{G_{m0}{}^2 P_{20}} \quad (91)$$

$$C_{tc} = \frac{G_{m0}(P_{30} - C_{tx})}{P_{60}} \quad (92)$$

$$C_{te} = \frac{(P_{60} - G_{m0})(P_{30} - C_{tx}) - P_{60}P_{10}}{(1 - 2P_{60}/G_{m0})P_{60}} \quad (93)$$

$$R_{cc} = \frac{P_{40} - (C_{tc} + C_{te})C_{tc}R_{bi}/12}{C_{tc}{}^2(1 - \frac{R_{bi}}{12R_{be}})} \quad (94)$$

$$\tau = \frac{P_{50}/G_{mo} + (C_{tc} + C_{te})R_{bi}/12}{\frac{R_{bi}}{12R_{be}} - 1} \quad (95)$$

where C_{tx} has been extracted in above cutoff mode and can be considered as a known quantity. By far the small-signal model parameters in the normal- operated intrinsic HBTs have been directly extracted. The proposed parameters extraction method will be verified in the following Section.

IV. RESULTS AND DISCUSSION

In order to validate the effectiveness of the proposed model and parameter extraction technique, SiGe HBTs under several bias conditions are investigated. The devices under test are fabricated by HuaHong Semiconductor Company in China.

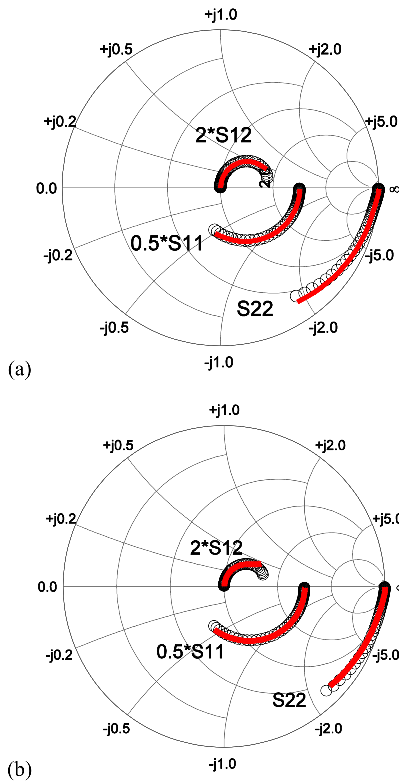

FIGURE 6. Comparison of measured and modeled data for a $1 \times 1.2 \times 30$ μm^2 SiGe HBT at (a) $V_{BE} = -1$ V, $V_{CE} = 0$ V and (b) $V_{BE} = 0$ V, $V_{CE} = 2$ V.

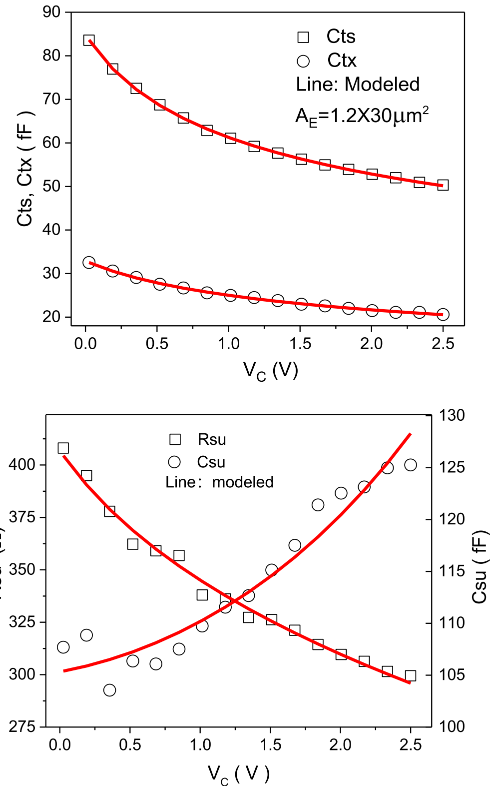

FIGURE 7. Bias dependence of extracted parameters of a $1 \times 1.2 \times 30$ μm^2 SiGe HBT.

An interdigital layout of 1E2B2C is adopted for chip design. The typical current gain cutoff frequency (f_T) is about 25 GHz and breakdown voltage BV_{CEO} is about 4.5 V. S-parameters were measured in the common emitter configuration with an on-wafer RF probe system and an Agilent PNA-X network analyzer over the frequency range of 100 MHz-20.89 GHz. The calibration was first performed on a ceramic calibration substrate using a short-open-load-thru calibration method. The pad parasitics were then de-embedded with a standard "open" and "short" structure from the measured S-parameters [11].

The measured S-parameters under cut-off state are first compared to the simulated data with distributed transmission line model in ADS simulator. The HBT structure was broken into 200 discrete transistors, similar to the case in Fig.1. The collector terminals of these transistors were connected together, and the base terminals from the two sides of the structure are also connected together. Two cutoff states (a) $V_{BE} = -1$ V, $V_{CE} = 0$ V and (b) $V_{BE} = 0$ V, $V_{CE} = 2$ V are investigated and depicted in Fig. 6. Good agreement is obtained over the whole frequency range from 100 MHz to 20.89 GHz, which demonstrates a high precision of our proposed extraction method.

Fig. 7 depicts the variation of extracted extrinsic capacitance C_{tx}, depletion layer capacitance C_{ts}, substrate resistance R_{su} and bulk capacitance C_{su} for a $1 \times 1.2 \times 30$ μm^2 SiGe HBT. The solid line is the empirical fitting by the theoretical C-V and R-V equation. The extracted model parameters match well with the modeled one over the whole bias range. Thus, the model parameters under arbitrary voltage can be determined and then de-embedded to extract the parameters at forward-active mode.

Fig. 8 depicts the comparison of measured and modeled S-parameters for $1 \times 1.2 \times 30$ μm^2 SiGe HBT at forward-active mode: $V_{BE} = 0.875$ V, $V_{CE} = 3$ V. To clearly reflect the quality of the agreement between measured and modeled data, the comparison of S-parameters in real and imaginary format is adopted. Excellent agreement exists over the whole frequency range. Table 3 lists the extracted parameters for two forward-active modes.

The residual error characterizing the accuracy between measured and modeled S-parameters is given as [11]

$$E = \frac{1}{4N} \sum\nolimits_{i=1}^{2} j = 1 \sum\nolimits_{k=1}^{N} \frac{|S_{ij}^{m}(f_k) - S_{ij}^{c}(f_k)|}{max_k |S_{ij}^{m}(f_k)|} \times 100\% \tag{96}$$

where N is the number of frequency. $S_{ij}^{mea}(f_k)$ and $S_{ij}^{sim}(f_k)$ are the measured and simulated S-parameters at the frequency f_k, respectively. The residual discrepancies are separately 1.79% and 1.86% for the two cases, which validates the accuracy of our proposed transmission line modeled and parameter extraction method.

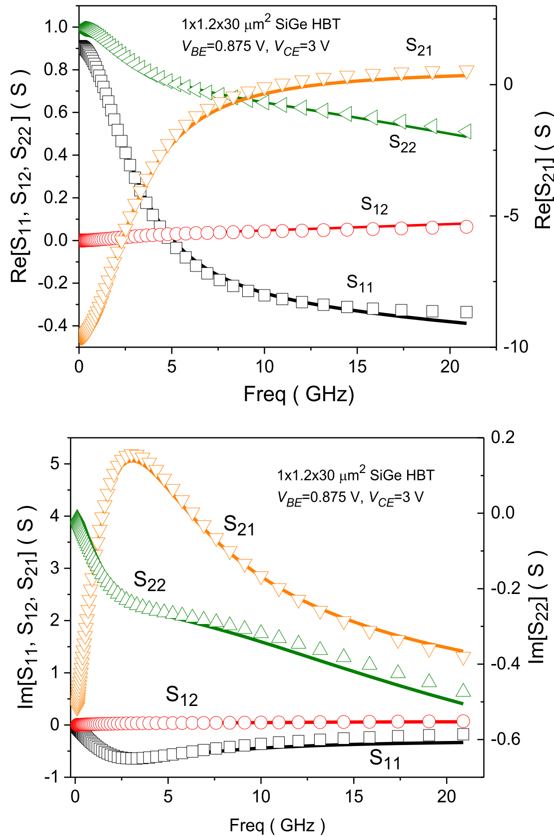

FIGURE 8. Comparison of S-parameter in RI form for $1 \times 1.2 \times 30\ \mu m^2$ SiGe HBT biased at $V_{BE} = 0.875$ V, $V_{CE} = 3$ V.

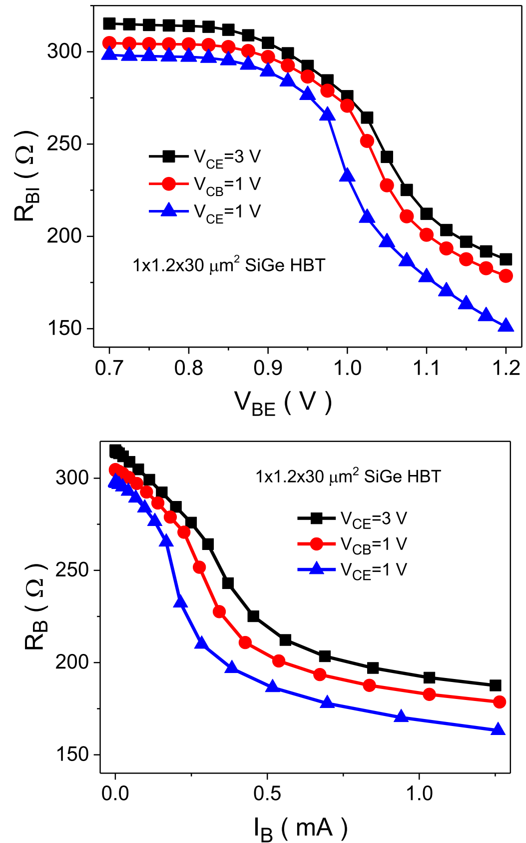

FIGURE 9. Bias dependence of extracted base resistance R_{BI} for a $1 \times 1.2 \times 30\ \mu m^2$ SiGe HBT.

TABLE 3. Extracted values of model parameters for $1 \times 1.2 \times 30\ \mu m^2$ SiGe HBT under (a)$V_{BE} = 0.875$ V and $V_{CE} = 3$ V, and (b)$V_{BE} = 0.875$ V and $V_{CE} = 1$ V.

Parameter	V_{BE}=0.875 V, V_{CE}=3 V	V_{BE}=0.875 V, V_{CE}=1 V
R_E (Ω)	2.0	2.0
R_{CX} (Ω)	5.44	5.44
R_{su} (Ω)	283.6	345
C_{ts} (fF)	47.98	61.27
C_{su} (fF)	138.28	110.17
C_{tx} (fF)	21.35	31.27
C_{tc} (fF)	5.5778	11.069
C_{te} (fF)	712.166	828.498
R_{be} (Ω)	835.971	895.978
R_{bi} (Ω)	308.88	292.936
R_{CC} (Ω)	68.5117	269.675
R_O (Ω)	10841	18181.8
G_{mo} (mS)	130.761	124.757
τ (ps)	0.497019	0.411718

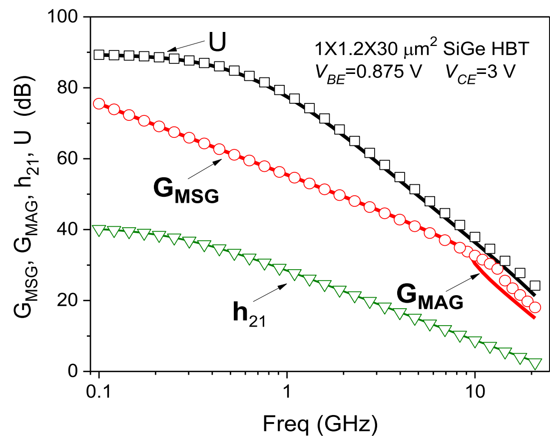

FIGURE 10. Comparison of the measured (symbols) and modeled (lines) h_{21}, G_{MSG}/G_{MAG}, U from 100 MHz to 20.89 GHz for a $1 \times 1.2 \times 30\ \mu m^2$ SiGe HBT at $V_{BE} = 0.875$ V, $V_{CE} = 3$ V.

S-parameter at other bias conditions are also compared and the results show that the modeled data all match well with the measured ones. The variation of extracted intrinsic base resistance R_{BI}, as function of V_{BE} and I_B, is presented in Fig. 9. As expected, due to the base broadening effect, the extracted R_{BI} decreases with I_B or V_{BE} increasing.

Fig. 10 depicts the comparison between the measured and modeled maximum stable gain G_{MSG}, maximum available gain G_{MAG}, unilateral power gain U and h_{21}. It can be seen that the extracted small-signal model parameters can accurately predict the power gain in the entire frequency. The maximum oscillation frequency (f_{max}) and current gain cutoff

frequency (f_T) can be obtained by extrapolating to U and h_{21} at a slope of 20 dB/decade. Therefore, we believed that the proposed transmission-line small-signal model and parameter technique are with high accuracy to evaluate fabricated process and optimize transistor design.

V. CONCLUSION

In this paper, we have developed an improved high frequency distributed small-signal model for SiGe HBTs. The transistor is divided into many infinitesimal cascade elements, and the admittance matrix of distributed network is derived by solving the transmission line equation. Through reasonable simplification of the admittance parameters, several constants are obtained based on the rational function fitting of the measured admittance parameters, and then the extrinsic and intrinsic model parameters are directly determined in a closed-form analytical expression separately, without any approximations and special test structures. The modeled and measured S-parameters depict an excellent agreement over a wide frequency range.

REFERENCES

[1] C. Coen, S. Zeinolabedinzadeh, M. Kaynak, B. Tillack, and J. D. Cressler, "A highly-efficient 138–170 GHz SiGe HBT frequency doubler for power-constrained applications," in *Proc. IEEE RFIC Symp.*, May 2016, pp. 23–26.

[2] E. Ojefors, J. Grzyb, Z. Yan, B. Heinemann, B. Tillack, and U. R. Pfeiffer, "A 820 GHz SiGe chipset for terahertz active imaging applications," in *IEEE ISSCC Dig. Tech. Papers*, Feb. 2011, pp. 224–246.

[3] M. Schröter and A. Chakravorty, *Compact Hierarchical Bipolar Transistor Modeling With HiCUM*. Singapore: World Scientific, 2010.

[4] J. C. J. Paasschens and W. J. Kloosterman, "The mextram bipolar transistor model level 504," Koninklijke Philips Electron., Delft, The Netherlands, Nat. Lab. Unclassified Rep. NL-UN 2000/811, 2001.

[5] J. C. J. Paasschens, "Compact modeling of the noise of a bipolar transistor under DC and AC current crowding conditions," *IEEE Trans. Electron Devices*, vol. 51, no. 9, pp. 1483–1495, Sep. 2004.

[6] S. Yadav, A. Chakravorty, and M. Schröter, "Small-signal modeling of the lateral NQS effect in SiGe HBTs," in *Proc. IEEE BCTM*, Sep. 2014, pp. 203–206.

[7] M.-Y. Chuang, M. E. Law, and K. O, "Three-dimensional base distributed effects of long stripe BJT's: Base resistance at DC," *IEEE Trans. Electron Devices*, vol. 45, no. 2, pp. 439–446, Feb. 1998.

[8] K. Xia, "Modeling the distributive effects of rc transmission line using recursive segmentation and applications to MOSFETs and BJTs," *IEEE Trans. Electron Devices*, vol. 63, no. 9, pp. 3385–3392, Sep. 2016.

[9] H. N. Ghosh, "A distributed model of the junction transistor and its application in the prediction of the emitter-base diode characteristic, base impedance, and pulse response of the device," *IEEE Trans. Electron Devices*, vol. ED-10, no. 12, pp. 513–531, Oct. 1965.

[10] J. Y. Hasani, "Modeling of distributed effects in modern MOS transistors for millimeter wave applications," *IEEE Trans. Electron Devices*, vol. 63, no. 3, pp. 925–932, Mar. 2016.

[11] S. Bousnina, P. Mandeville, A. B. Kouki, R. Surridge, and F. M. Ghannouchi, "Direct parameter-extraction method for HBT small-signal model," *IEEE Trans. Microw. Theory Techn.*, vol. 50, no. 2, pp. 529–536, Feb. 2002.

[12] A. Oudir, M. Mahdouani, and R. Bourguiga, "Direct extraction method of HBT equivalent-circuit elements relying exclusively on *S*-parameters measured at normal bias conditions," *IEEE Trans. Microw. Theory Techn.*, vol. 59, no. 8, pp. 1973–1982, Aug. 2011.

[13] Y. Sun *et al.*, "An improved small-signal model for SiGe HBT under off-state, derived from distributed network and corresponding model parameter extraction," *IEEE Trans. Microw. Theory Techn.*, vol. 63, no. 10, pp. 3131–3141, Oct. 2015.

[14] J. C. J. Paasschens, W. J. Kloosterman, and R. V. D. Toorn, "Model derivation of Mextram 504. The physics behind the model," Koninklijke Philips Electron., Delft, The Netherlands, Nat. Lab. Unclassified Rep. NL-UR 2002/806, 2002.

[15] J. Yang *et al.*, "Novel extraction of emitter resistance of SiGe HBTs from forward-Gummel measurements," in *Proc. IEEE EDSSC*, Jun. 2014, pp. 1–2.

[16] R. Gabl and M. Reisch, "Emitter series resistance from open-collector measurements-influence of the collector region and the parasitic pnp transistor," *IEEE Trans. Electron Devices*, vol. 45, no. 12, pp. 2457–2465, Dec. 1998.

[17] C. Raya, T. Schwartzmann, P. Chevalier, F. Pourchon, D. Celi, and T. Zimmer, "New method for oxide capacitance extraction," in *Proc. IEEE BCTM*, Sep. 2007, pp. 188–191.

YABIN SUN received the B.S. degree in electrical engineering from Jilin University, Changchun, China, in 2010, and the Ph.D. degree in electrical engineering from Tsinghua University, Beijing, China, in 2015.

In 2016, he joined the Department of Electrical Engineering, East China Normal University, Shanghai, China, as a Lecturer. His current research interests focus on microwave device design, characterization, and modeling.

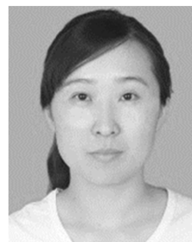

ZIYU LIU received the B.S. degree in material science and engineering from Jilin University, Changchun, China, in 2010, and the Ph.D. degree in electrical engineering from Tsinghua University, Beijing, China, in 2016.

From 2016 to 2018, she was a Research Assistant with the Centre for Biosystem, Neuroscience and Nanotechnology, Department of Electronic Engineering, City University of Hong Kong, Hong Kong. Since 2018, she has been with the State Key Laboratory of ASIC and System, School of Microelectronics, Fudan University. Her research interests include semiconductor process, device, and model.

XIAOJIN LI received the B.S., M.S., and Ph.D. degrees from East China Normal University, Shanghai, China, in 2001, 2004, and 2009, respectively, all in electrical engineering.

He had a short-term learning experience in electrical engineering with National Tsing Hua University, Hsinchu, Taiwan, in 2008. He is currently an Associate Professor in electrical engineering with East China Normal University. His research interests include IC circuit design and device reliability modeling.

YANLING SHI received the B.S., M.S., and Ph.D. degrees from East China Normal University, Shanghai, China, in 1990, 1993, and 2002, respectively, all in electrical engineering.

In 2004, she was an Engineer with imec, Belgium. During this time, she participated in the development of 90-nm CMOS process. She is currently a Professor in electrical engineering with East China Normal University. Her research interests include CMOS device and modeling.